Rahnejat, H., "An introduction to multi-physics multi-scale approach", in Rahnejat, H (Ed.), Tribology and dynamics of engine and power train, Woodhead Publishing, Cambridge, UK, 2010, ISBN: 978-1-84569-361-9

An introduction to multi-physics multi-scale approach

H. Rahnejat
Wolfson School of Mechanical & Manufacturing Engineering, Loughborough University, Loughborough, UK

Nomenclature:

a : Acceleration
C_{ij} : Constraint function
E : Young's modulus of elasticity
F : Force
F_{a^j} : Applied forces
F_{q^j} : Generalised body forces
g : Gravitational acceleration
G : Universal gravitational constant
h : Conjunctional film thickness
I_{q^j} : Mass moments of inertia
ℓ : Characteristic "size" of a system
L : Length of Eulerian beam
k : Stiffness
K : Kinetic energy
m : Mass of a material point
M : Mass of a source
p : Pressure
P : Momentum
q^j : Generalised co-ordinates (usually Eulerian 3-1-3 body-centred rotations)
r : Distance from a source or local position vector
R : Global position vector
u, v : Conjunctional velocities of flow
U : Potential energy
t : Time
$[T], [T^*]$: Transformation matrices between sets of co-ordinates
x, y, z : Cartesian co-ordinates
δ : Deflection/deformation
δq : Small change in co-ordinate q
ε : "size" of a generic material point
ϕ : Potential
η : Dynamic viscosity
λ : Lagrange multiplier

ρ : Density

ξ^j : Global co-ordinates in reduced configuration space

ψ, θ, φ : Euler angles

Subscripts:

a^i : Applied in the co-ordinate i

q^j : Refers to a generalised co-ordinate

Superscripts:

i, j, k, l : Refer to sets of co-ordinates

T : Transposed

. : First time derivative

.. : Second time derivative

Other symbols:

$\sum$: Summation

$\bullet$: Vector dot product

$\in$: Inclusive of

1.1- Introduction

Dynamics and tribology, described in this book, may be regarded as subsets of physics of motion (in a multi-physics perspective). Dynamics is the study of motion of entities caused by the underlying forces. Historically, in the discipline of dynamics and within engineering these entities have been considered to be assembly of parts (a system), solid inertial elements (a component) and rigid particles. When the study of motion of a ***material point*** (a generic term used to describe these entities; a particle, a body: a conglomerate of such particles or a system: an assembly or cluster of bodies) is observation-based only (without regard to the underlying cause: force), then the field of investigation is referred to as ***kinematics***. In the case of a multi-body or a many-body system, kinematics refer to studies with no degrees of freedom; relative motions between their constituent material points (their motion is pre-specified).

When a system undergoes no displacements with respect to a specified frame of reference (a co-ordinate set; *t, x, y, z*), then it is regarded to be ***static***. The forces applied to such a system are said to be in a state of equilibrium (no net force). If a multitude of such equilibria can be assumed, then these various states of the system may be termed as ***quasi-static***.

Real systems are not rigid. An example is the power train system, subject of this book, where hollow driveshaft tubes undergo small amplitude elastic deformation under load, whilst they undertake much larger inertial motions (see chapter 30, explaining the clonk phenomenon). The same is true of all

material points, although in many cases, such as molecules, the deformation would be infinitesimal and thus almost insensible. Therefore, flexible systems are subject to ***elastodynamics***. Since the deformation amplitudes are different in scale of measurement to the overall inertial displacements, the problem is ***multi-scale***. If one disregards the larger scale and the study is confined to small amplitude oscillations, then the problem at hand is regarded as one of ***vibration***. In general all real material points, being compliant, can assume many forms when vibrating. These forms are known as modes. For example, chapter 30 shows various modes of flexible driveshaft tubes. The same is true of very small material points such as electrons with their wavy motions with many spins. At the other end of scale, it is surmised that even heavenly bodies pulsate or quiver, spreading waves on the fabric of space, rather similar to the wave propagation on the surface of driveshaft tubes, explained in chapter 30.

When undertaking study of a problem in dynamics, the boundary of the system must be defined, because there is no generic system. The interactions between the defined system and those material points extraneous to it are then ignored. This is a fundamental rule of experimentation. Thus, for example, in vehicle engineering, problems are defined as those of the power train system or vehicle-road interactions, and not a vehicle within the universe! With the system boundaries defined, interaction of key material points are considered. These interactions are simply forces acting between them, causing motions in a multitude of physical scales. Therefore, the interaction scale(s) of interest should also be determined. For example, power train dynamics problems may be in the scale of large displacements (inertial dynamics: shuffle, see chapters 21, 23 and 30) or structural response (modal behaviour of driveshaft tubes or the transmission case, see chapter 30) or noise propagation (acoustic response of thin walled structures). These may be regarded as wave motions from scales of metres to sub-millimetre and onto nanometres respectively, but they are all part of dynamics of a defined system (so are the usual micro-scale deflections of load bearing conjunctions in tribology, see chapters 4, 5 and 6). The environment outside the system boundary is considered to be rigid, to which a global frame of reference for measurement of multi-scale physics of motion is firmly attached (Rahnejat, 1998). In reality the extraneous environment is not rigid, nor any place within the known or surmised universe. The experiment carried out in a laboratory within a defined system is positioned on Earth which moves around the Sun at 66730 miles/hr (average), whilst the Solar system is dragged by the Sagitarius A* at the centre of the Galaxy at 45000 miles/hr towards the constellation of Hercules. However, one can consider the dominant forces in the experiment to be because of material points of the defined system and in some cases (bodies of significant size) due to the Earth gravitational pull only. Thus, in dynamics the motion of a material point is governed by all those within the same system. This is the essence of ***Mach's principle*** and is fundamental to the subject of dynamics. Now with this philosophical basis and within any system of any conglomerate of material points i , any one such point has an acceleration due to its interactions with others as:

$$a = \frac{\sum_i F_i}{m} \tag{1.1}$$

This is ***Newton's second law*** of motion, where *m* is the mass of any material point. Newton called this an axiom, because in his perspective it was a natural observation for which no proof was required at the time of his enunciation, same as Euclid's geometrical axioms. The second law is the foundation upon which all the field of dynamics resides. Later a fundamental proof for this axiom is provided through energy consideration; Lagrange's equation.

The notion of material points is not confined to those of a solid nature, but all matter in any physical state including fluids. Thus, a system may be defined as a volume of fluid bounded by solid surfaces such as a river and its impervious banks. The volume of fluid may be considered as a series of elemental volumes progressing through the system in the same manner (but not exactly) as the deformation wavefronts progress in the hollow driveshaft tubes in chapter 30. The study is, therefore, one of continuous fluid flow due to a pressure gradient and velocity profile (both as a result of forces) through the assumed system. The subject is called ***hydrodynamics*** (see chapter 5). This is also a multi-scale problem, same as other forms of dynamics. For a large expanse of fluid, the elemental volumes may be considered large, but finite within which a state of equilibrium may be assumed relative to the interactions between any pair of such elements themselves. Large elemental volumes mean significant body forces (weight) and inertial forces. On the other hand, in tribological conjunctions, narrowness of gap between the boundary solids means small elemental volumes and their assumed uniform motion through the system (the conjunction). Thus, the problem simplifies to that of flow induced by changes in pressure gradient and any relative motion of bounding surfaces, forming a ***wedge effect*** (Gohar and Rahnejat, 2008, also see chapter 5). Therefore, the complex flow dynamics is reduced to a manageable problem in hydrodynamics, with a fundamental equation:

$$\frac{\partial}{\partial x}\left(\frac{\rho h^3}{12\eta}\frac{\partial p}{\partial x}\right)+\frac{\partial}{\partial y}\left(\frac{\rho h^3}{12\eta}\frac{\partial p}{\partial y}\right)=u\frac{\partial \rho h}{\partial x}+v\frac{\partial \rho h}{\partial y}+\frac{\partial \rho h}{\partial t} \tag{1.2}$$

Reynolds obtained this equation by ignoring the effect of surface, body and inertial forces for small incremental elemental volumes of fluid, confined by a pair of close solid boundaries (chapter 5 describes the equation in detail). Therefore, as in the case of solids, a question of scale exists in the case of fluids as well. If the size of the system is reduced, the incremental *computational* volume must also decrease accordingly, where the conditions within such a volume may be considered to be in equilibrium. It is, therefore, clear that in the extreme cases (ultra-thin film tribology) with molecular interactions and surface energy effects no bulk properties such as a computational elemental volume may be assumed (see chapter 3).

Therefore, one may surmise that physical interactions regardless of the state of matter are functions of size of the assumed system and that of a material point considered, or the ratio: ε/ℓ (Rahnejat, 2008). It turns out that the nature of physical interactions (force) changes according to scale (the same ratio). However, the size of the material point ε is explained by a host of physical attributes such as mass or charge and that of the system ℓ by density, viscosity, permittivity, elasticity, coefficient of friction, etc. This means that forces other than gravity are related to kinematic quantities (displacement, velocity and acceleration) by physical properties of material points and the environment of the system. The introduction to chapter 3 describes the philosophical concern about the multiplicity of forces of Nature. This means the current knowledge is based on acceptance of a multi-physics character for interactions of material points at multi-scale within defined systems, thus the increasingly used phrase: ***multi-scale multi-physics analysis***. Finally, this brief introduction has shown that both dynamics and tribology are subsets of physics of motion.

1.2- Newtonian Mechanics

Kinematics, being the study of motion without regard to the underlying cause (force), is one of the oldest sciences. Its roots can be traced back to the ancient studies of heavenly bodies, such as Homer's Earth-centred Universe in the *Iliad*. As an observation-based science, ***kinematics*** is concerned with measurement of the state of motion of a material point (displacement, velocity and acceleration) with respect to a frame of reference. As already discussed, it is particularly convenient to firmly attach this frame of reference to a fixed (static) object. Therefore, it was particularly convenient to assume Earth to be the fixed central entity about which all the heavens would revolve (presumably in the adoration of humanity!). The heavenly bodies would then describe curvilinear paths whose slope at a given position yield their relative velocity with respect to the frame of measurement. Much later, Galileo understood that deviation from a straight line motion corresponded to non-uniform velocity and the curvature was due to accelerated motion. Therefore, kinematics is the study of curves; their local slope and curvature. By late 16^{th} and early 17^{th} centuries kinematics had finally attained the status only hitherto afforded to geometry as a fundamental science, because of the historical prominence of ancient and middle-ages' geometers such as Homer, Pythagoras, Archimedes, Ptolemy, Khayam, Tusi and Copernicus, among others. Using astronomical observations and a cursory understanding of non-uniform motion, Galileo and Kepler put an end to the concept of Earth-centred Universe and obviously a sizeable dent in the human vanity! Kinematics had its greatest moment in history with the acceptance of the ***heliocentric system***.

Using Kepler's observations and his laws of motion, Newton explained the elliptical orbit of planets around the Sun by a central force due to gravitational attraction. The cause belying kinematics was found; force. In the case of planetary motions, the force of gravity caused the non-uniform accelerated motion; curvature of the path. The law of Universal Gravitation states:

$$F = \frac{GMm}{r^2} = mg \tag{1.3}$$

where *G* is the ***universal gravitational constant***, *M* mass of a source (such as the Sun) and *m* that of a target body (such as Earth). Thus, the radius of curvature *r* at any position along the path is $r = \sqrt{\frac{GM}{g}}$ for a 2-body system (Sun and Earth). Since the Earth's path is elliptical (only slightly) on the Ecliptic plane, then *r* is not a constant, which means that g varies accordingly.

The simple calculations here assumes a 2-body system, but path of a body within a system (Earth in the Solar system) is subject to all material points within it (other planets), remember the Mach's principle. More comprehensive treatment of this problem is given by Chandrasekhar (1995).

Newton then stated that in general equation (1.3) can be extended to his second axiom; equation (1.1). If there is no net force; $F = 0$, a body at rest remains stationary, whilst one in motion pursues a straight line path; ***Newton's first axiom***. A straight line path is an extremal path (shortest path) due to uniform motion of a material point relative to an observer. One can surmise from equation (1.3) that attraction between two bodies necessitates equal and opposite forces. This is ***Newton's third axiom***; for every action there is an equal and opposite reaction.

The assertion of these axioms by Newton, in addition to the law of universal gravitation, resulted in scientific disputes, some of which persisted beyond his lifetime. One concerned a fundamental proof for the second axiom, to render the same as a law of physics. An ***axiom*** is an assertion which appeals to all observers who would all agree on the cause of a phenomenon. This definition does not put the onus of acceptance on a mathematical proof; such as the existence of the Sun. Some have proposed intangible proofs for certain axiomatic concepts such as Descartes' for "life": *I think, therefore, I am*. Mathematical discourse has increasingly been viewed as a requirement for proof since the 17th century. In this respect, ***Lagrange's equation*** is the proof of Newton's second axiom as:

$$\frac{d}{dt}\left(\frac{\partial K}{\partial \dot{q}^j}\right) + \frac{\partial U}{\partial q^j} = F_{a^j} \tag{1.4}$$

where K is the kinetic energy (considered to be independent of displacement q with the right choice of co-ordinate system), *U* is the potential energy and F_{a^j} the component of net applied force in the co-ordinate direction q^j (a generalised proof is given in section 1.3).

In general a completely unconstrained material point in space has 6 degrees of freedom, therefore, the generalised co-ordinate set: $q^j \in x, y, z, \psi, \theta, \varphi$. The ***kinetic energy*** has, therefore, components: $K_j = \frac{1}{2} m \dot{q}^{j^2}$ for the translational degrees of freedom and $K_j = \frac{1}{2} I_{q^j} \dot{q}^{j^2}$ for rotational ones. Therefore, it can be seen that the first term on the left-hand side of Lagrange's equation is the inertial force, for example for $q^j = x$:

$$\frac{d}{dt}\left(\frac{\partial K}{\partial \dot{x}}\right) = \frac{d}{dt}\left(\frac{\partial\left(\frac{1}{2} m \dot{x}^2\right)}{\partial \dot{x}}\right) = \frac{d(m\dot{x})}{dt} = m\ddot{x} \qquad (1.5)$$

Now, the second term on the left-hand side of Lagrange's equation is the ***Euler's equation***, simply stating that the rate of change of ***potential energy*** with respect to displacement is the body or restoring force:

$$F_{q^j} = -\frac{\partial U}{\partial q^j} \qquad (1.6)$$

Thus, a material point falling freely under the influence of gravity towards the centre of Earth from any height x, with the frame of reference q aligned with the direction of motion has a body force:

$$F_x = -\frac{\partial(mgx)}{\partial x} = -mg \qquad (1.7)$$

Using Lagrange's equation and noting that there is no applied force (free fall); $F_{ax} = 0$, then: $F_{ax} = m\ddot{x} - mg$ ($\ddot{x} = g$), which is Newton's second axiom. Therefore, Lagrange's equation is essentially the determination of net force, causing an acceleration (same as equation (1.1)):

$$a_q = -\frac{\partial \phi}{\partial q} = \frac{1}{\Omega}\left\{F_{aq} - \frac{\partial U}{\partial q}\right\} \qquad (1.8)$$

where: $\Omega \in m, I$ according to the degree of freedom (translational or rotational). Thus, if a potential ϕ can be specified, then acceleration of all

material points within such a field can be determined. One can now revisit the same example of the falling matter above, this time attaching the frame of reference to the material point itself, falling within a field, where: $\phi = -\frac{GM}{x}$. In this case, $q = x$, $\Omega = m$, $F_{ax} = 0$ as before and $a_q = \ddot{x}$, then:

$$\ddot{x} = \frac{GM}{x^2} = g \qquad (1.9)$$

which yields the same results as previously. Two important observations should be made. Firstly, the potential used is due to gravitation, thus equation (1.3) is proven from first principles. If the field is due to Earth's gravity then *M* represents its mass. $x = r + H$ is the distance to the centre of Earth, r its radius and h the height of the falling matter above the Earth's surface. Since usually: $H << r$, g hardly changes near the surface of Earth. This justifies the use of a constant value for g in engineering. Secondly, the above alternative analyses yield the same result, indicating the equivalence of the two systems; one in a gravitational field and the other falling uniformly with an equivalent inertial acceleration. This was noted by Einstein as the ***equivalence principle***, the implication being that inertial acceleration produces gravitational action. There are many examples, such as a material point in curvilinear motion or planetary motion or a vehicle cornering. This means that motion on curves induces gravitational action. This became clear with Einstein's general relativity; after all physics of motion in all its forms could be reduced to study of curves and motion of material points upon them. This appears to be true apart from various electromagnetic phenomena in the scale of minutiae as described in chapter 3. The problem is that general relativity is based on a theory for gravity (macroscopic material points), Thus, seemingly prevalent potentials at very small scale deviate from it. The next section discusses Lagrange's equation. Readers should note that inertial and body forces which are dominant in the equation play an insignificant role in the scale of minutiae (see also chapter 3).

1.3– Lagrange's Equation and Reduced Configuration Space

The ***Lagrange's equation*** (1.4) is for unconstrained systems, where any material point within the defined system enjoys 6 degrees of freedom as already indicated above. However, recall that acceleration of a material point within a defined system is due to all other such points present (Mach's principle). Therefore, the defined system may be regarded as a ***reduced configuration space***, where motion of material points are restricted by their interactions (***constrained system dynamics***).

Newton's second axiom in any co-ordinate direction q may be presented in the form: $-F_{q^i} + m_{q^i}\ddot{q}^i = 0$. This form of equation simply states that any applied

external force on a material point m_{q^i} must be balanced by its inertial response. This form of second axiom is known as the ***D'Alembert's Principle*** (Rahnejat, 2008). Johannes Bernoulli extended D'Alembert's Principle to the net ***virtual work done*** for an n cluster of unconstrained material points, having $3n$ co-ordinates as: $\sum_{i=1}^{3n}(-F_{q^i} + m_{q^i}\ddot{q}^i)\delta q_i = 0$. If now there exists l constrained co-ordinates, then the reduced configuration space is: $r = 3n - l$. A new set of co-ordinates ξ is chosen, last l of which are constrained. Then, the ***holonomic constraints*** are:

$$q^i|_{i=1,3n} = f(\xi^j|_{j=1,r}, t) \text{ and } \xi^j|_{j=r+1,3n} = f(q^i|_{i=1,3n}, t) = 0 \qquad (1.10)$$

Then, the infinitesimal change in a co-ordinate is: $\delta q_i = \sum_j \frac{\partial q^i}{\partial \xi^j}\delta\xi_j$. Now replacing in the above expression for the virtual work done:

$$\sum_i \sum_j (-F_{q^i} + m_{q^i}\ddot{q}^i)\frac{\partial q^i}{\partial \xi^j}\delta\xi_j = 0 \qquad (1.11)$$

This can be written in the form:

$$\sum_i \sum_j (m_{q^i}\frac{\partial q^i}{\partial \xi^j}\ddot{q}^i - F_{q^i}\frac{\partial q^i}{\partial \xi^j})\delta\xi_j = 0 \qquad (1.12)$$

Since the co-ordinates ξ^j, velocities $\dot{\xi}^j$ and time are considered as independent variables, the first term can be written as:

$$\sum_j m_{q^i}\frac{\partial q^i}{\partial \xi^j}\ddot{q}^i = \frac{d}{dt}\left(\sum_j m_{q^i}\frac{\partial q^i}{\partial \xi^j}\frac{dq^i}{dt}\right) - \sum_j m_{q^i}\frac{dq^i}{dt} - \frac{d}{dt}\left(\frac{\partial q^i}{\partial \xi^j}\right) \qquad (1.13)$$

and the second term as: $\sum_i F_{q^i}\frac{\partial q^i}{\partial \xi^j} = -\sum_i \frac{\partial U}{\partial q^i}\frac{\partial q^i}{\partial \xi^j} = -\frac{\partial U}{\partial \xi^j}$ (1.14)

To simplify the above terms one needs the derivatives: $\frac{dq^i}{dt}$ and $\frac{\partial \dot{q}^i}{\partial \dot{\xi}^j}$. The latter is the same as $\frac{\partial q^i}{\partial \xi^j}$ and is substituted by it in the first term of (1.13). The former can be obtained from the constraints in (1.10). If the constraints are considered as time-dependent for an evolving system as would be the general case, then the absolute derivative ***(covariant vector*** for space-time***)*** is:

$$\frac{dq^i}{dt} = \frac{\partial q^i}{dt} + \sum_i \frac{\partial q^i}{\partial \xi^j}\frac{d\xi^j}{dt} \tag{1.15}$$

These can all be substituted back into (1.13) and (1.14), completing equation (1.12). One additional clarification is for the second term in (1.13), where:

$$\frac{d}{dt}\left(\frac{\partial q^i}{\partial \xi^j}\right) = \frac{\partial^2 q^i}{\partial \xi^j \partial t} + \sum_k \frac{\partial^2 q^k}{\partial \xi^j \partial \xi^k}\frac{d\xi^k}{dt} = \frac{\partial}{\partial \xi^j}\left(\frac{dq^i}{dt}\right).$$

After all the indicated substitutions and some manipulation, equation (1.12) becomes:

$$\sum_i \left\{ \frac{d}{dt}\sum_j m_{qi}\frac{\partial q^i}{\partial \xi^j}\underbrace{\left(\frac{\partial q^i}{\partial t} + \sum_i \frac{\partial q^i}{\partial \xi^j}\frac{d\xi^j}{dt}\right)}_{\frac{dq^i}{dt}} - \sum_j m_{q^i}\underbrace{\left(\frac{\partial q^i}{\partial t} + \sum_i \frac{\partial q^i}{\partial \xi^j}\frac{d\xi^j}{dt}\right)}_{\frac{dq^i}{dt}}\left(\frac{\partial \dot{q}^i}{\partial \xi^j}\right) + \frac{\partial U}{\partial \xi^j}\right\}\delta q_i = 0 \tag{1.16}$$

Since, $\delta q_i \neq 0$, then the term in the curly bracket must vanish. As kinetic energy $K = \frac{1}{2}\sum_i m_{q^i}\left(\frac{d\dot{q}^i}{dt}\right)$, then it is clear that the first term in the bracket is $\frac{\partial K}{\partial \dot{\xi}^j}$ and the second term is $\frac{\partial K}{\partial \xi^j}$. Thus:

$$\frac{d}{dt}\left(\frac{\partial K}{\partial \dot{\xi}^j}\right) - \frac{\partial K}{\partial \xi^j} + \frac{\partial U}{\partial \xi^j} = 0 \tag{1.17}$$

This is a more general form of the ***Lagrange's equation*** than (1.4). The time dependent holonomic constraints are taken into account, which means that for such a system the set of equations are for $j = 1 \to r$. A solution for the defined system of n material points is thus obtained for this set of differential equations with the holonomic constraints $\xi^j{}_{|j=r+1,3n} = f(q^i{}_{|i=1,3n}, t) = 0$ (as described above). As it can be seen, the holonomic constraints are relationships that forbid displacements along or about certain defined co-ordinates. The derivation here assumes these constraints to be time dependent. In most engineering applications holonomic constraints are time independent. This means that the first term on the left-hand side of the velocity transform in (1.15) does not exist. This leads to a ***contravariant velocity vector***.

Constraints may be ***non-holonomic***, such as velocity dependency of pairs of co-ordinate systems. Readers should refer to specialist texts on multi-body

dynamics (e.g. Rahnejat, 1998). If a co-ordinate system is fixed onto the ground in a gravitational field and another falls with respect to it, then the relationship between them can be described by non-holonomic constraints as co-ordinate functions of the gravitational field.

The simple derivation of Lagrange's equation here suffices, both for mathematical proof of Newton's second axiom and for use in mechanical problems. Many other formulations of Lagrange's equation can be arrived at, which suit particular systems or aid certain solution methods. Readers should refer to Orlandea (1999).

Multi-body mechanical systems as assembly of parts are viewed as constrained system dynamics problems. Such systems comprise a number of components that, in general, are referred to as *parts*. Parts are joined together by constraint functions which provide relationships between co-ordinates attached to certain points on these neighbouring parts (similar relationships in equation (1.10)). These points are known as *markers*. In mechanical systems there are an assortment of joints, such as hinge/revolute, ball-in-socket/spherical, hook/universal, cylindrical, translational, and more complex joints such as various constant velocity joints, clevis joint, to name but a few. An introduction to mechanical joints may be found in Rahnejat (1998), Hunt (1973) and Gilmartin (1978).

In general, each mechanical joint introduces a number of constraints (i.e. a series of relationships between co-ordinates attached to the aforementioned *markers*). These provide a number of algebraic equations which must be satisfied simultaneously with differential equations of motion of *parts* (application of Lagrange's equation for various degrees of freedom of each part) within a multi-body system. Various solution methods for such sets of differential-algebraic equations in space-time exist. Again readers should refer to Rahnejat (1998) or Orlandea (2008).

1.4- Multi-body Mechanical Systems

1.4.1- Equations of Motion

Mechanical systems, including engine and power train systems are constrained multi-body systems. At first sight many practical mechanical multi-body systems appear to be quite complex when a dynamic model, comprising a differential-algebraic set of equations is to be made. However, this task is made quite simple by commercial software, many of which generate the set of equations for the user in an automatic manner. In order to achieve this, Lagrange's equation for constrained systems may be stated in the form:

$$\frac{d}{dt}\left(\frac{\partial K}{\partial \dot{q}^i}\right)+\frac{\partial U}{\partial q^i}+\sum_m \lambda_m \frac{\partial C_{kl}}{\partial q^i}=F_{aq^i} \qquad (1.18)$$

where the constraint functions $C_{kl}, k=1,n$ and $l=1,n$ with $k \neq l$ are functions of co-ordinates of *markers* on *parts* $(1,n)$ in the multi-body system and λ_m are ***Lagrange multipliers*** for m constraints applied to a *part*, which are unknowns to be determined.

To obtain the equation set, it is usual to define a fixed co-ordinate system with respect to which all translational and rotational motions of *parts* within a multi-body system are measured. This fixed frame of reference is usually referred to as the ***global frame of reference***. It is global in the sense that all the motions of other frames of reference attached to individual components of a multi-body system undergo transformations with respect to it. Recall, from previous discussion that a generic global frame of reference cannot be assumed anywhere, unless within an isolated suitably defined system of investigation. The co-ordinates fixed to each *part* of the system are referred to as ***local part frame of reference***. If the *parts* are considered to be rigid and such frames of reference are attached suitably to their centres of mass/inertia, then the kinetic energy remains a function of $\dot{q}^i$ only and the form of Lagrange's equation (1.18) holds true for all parts in the multi-body system.

Transformation between a triad of axes in a local part frame of reference (LPRF) and the global frame of reference (GRF) is required in order to determine the kinematic attributes of the part in an instantaneous manner (in other words the GRF is the frame of observation). The kinematic observation model is, therefore, $q^i, \dot{q}^i$ for all parts i, whilst the dynamics model includes the underlying causes (forces); inertial: $\frac{dP_i}{dt}$ (P_i being the momentum conjugate to the co-ordinate q^i), the generalised body/ restoring/resistive force: F_{q^i}, the constraint reactions: $\sum_m \lambda_m \frac{\partial C_{kl}}{\partial q^i}$ and any applied forces. For known inertial properties and constraint functions (type of mechanical joints), the vector of unknowns in a multi-body mechanical dynamic system becomes: $\left\{q^i, \dot{q}^i, \lambda_j\right\}^T_{\in i,j}$. A noteworthy point is that whilst $F_{q^i} = -\frac{\partial U}{\partial q^i}$ may be regarded as a restraint (a resistance), the term $\sum \lambda_i \frac{\partial C_{kl}}{\partial q^i}$ is a constraint (a rigid restraint) determining the reduced configuration space. Thus, in mechanical systems stored energy in a linear spring $\frac{1}{2}k\delta^2$ by virtue of its deflection δ or that in a solid elastic sphere $\frac{2}{5}k\delta^{5/2}$ (see chapter 4) account for resistance in certain co-ordinates, whilst constraints C_{kl} define the limit of a dynamic system in relative motion of parts *k* and *l*. Constraints, therefore, remove the working space of mechanisms (a reduced configuration space).

Although constraints are often used in multi-body formulation, they represent rigidity that is idealistic. Recall that there exists no rigid location is space-time, to which one can attach a frame of reference. Constraints, therefore, have the dual purpose of problem simplification (when warranted) or to achieve kinematic conditions, where observation of articulation of a mechanism is deemed as a prelude to a later more detailed dynamic analysis (see Rahnejat, 1998).

To capture the position and orientation of an LPRF with respect to GRF it is usual to use roll-pitch-yaw transformations (common in aircraft and ship dynamics) or Euler's body 3-1-3 frame of reference (successive rotations of the embedded LPRF, a generalised form extensively used since Euler).

Now in a multi-body system the GRF is fixed on the ground, LPRFs are attached to the centres of mass/inertia of the moving bodies (the material points). The position vector of the origin of LPRFs $\left(q^i, i=1,6\right)_{k=1,n}$ with respect to the GRF $\left(\xi^j, j=1,6\right)$ are given as: $\{R_k\}_{k=1,n} = \left\{\left\|\xi^j\right\|_k, j=1,3\right\}^T \{\xi^1 \xi^2 \xi^3\}$. LPRFs assume varying orientations with respect to the GRF as system dynamics evolves in time. When the equations of motion are written for each part with respect to the respective embedded LPRF, it is necessary to have the Euler transformations from GRF to these:

$$\left\{q_k^i, i=1,3\right\}^T = [T]_k \left\{\xi^j, j=1,3\right\}^T \tag{1.19}$$

where the ***Euler transformation*** matrix is:

$$[T] = \begin{bmatrix} C\psi C\varphi - S\psi C\theta S\varphi & -C\psi S\varphi - S\psi C\theta C\varphi & S\psi S\theta \\ S\psi C\psi + C\psi C\theta S\varphi & -S\psi S\varphi + C\psi C\theta C\varphi & -C\psi S\theta \\ S\theta S\varphi & S\theta C\varphi & C\theta \end{bmatrix} \tag{1.20}$$

where: $C \equiv \cos, S \equiv \sin$. Also note: $\xi^4 = \psi, \xi^5 = \theta, \xi^6 = \varphi$ are the ***Euler angles*** in the Euler body 3-1-3 frame of reference.

The translational components of velocity of any *part* are given as: $\{v_k\}_{k=1,n} = \left\{\frac{\partial R_k}{\partial t}\right\}_{k=1,n} = \left\{\left\|\frac{\partial \xi^j}{\partial t}\right\|_k, j=1,3\right\}^T \{\xi^1 \xi^2 \xi^3\}$.

In the Euler's frame of reference rotations of an LPRF relative to the GRF are given as: $\left\{\dot{\xi}^j, j=4,6\right\}^T = \left\{\dot{\psi}, \dot{\theta}, \dot{\varphi}\right\}^T$. Rotational kinetic energy is obtained in terms of derivatives of LPRF co-ordinates: $\dot{q}^i, i=4,6$. These are transformed to the global frame of reference as: $\left\{\dot{q}^i, i=4,6\right\}^T = \left[T^*\right]\left\{\dot{\psi}, \dot{\theta}, \dot{\varphi}\right\}^T$,

where (Rahnejat, 1998): $\left[T^*\right]=\begin{bmatrix} S\theta S\varphi & 0 & C\varphi \\ S\theta & 0 & -S\varphi \\ C\theta & 1 & 0 \end{bmatrix}$ with co-directed ξ^3 and q^3 axes. Now simply replace q^i by ξ^j in equation (1.18) to find 6 equations of motion for each *part* (in figure 1.1) in the reduced configuration space defined by any algebraic constraint functions that join the *parts* of the multi-body system in terms of the global co-ordinates; GRF.

1.4.2- Constraint Functions

The equations of motion for any constrained mechanical multi-body system require definition of the ***constraint functions*** C_{kl} in terms of the co-ordinates ξ^j. Mechanical joints, such as those mentioned above compose of a number of basic algebraic functions, usually referred to as ***primitive constraints***. Such constraints are usually imposed between two *parts* in a system at a specific geometric location, which is defined by points (*markers*) on a pair of assembled *parts*. Rahnejat (1998) provides detailed treatment of mechanical joints' constraint formulation. Here a brief introduction to the subject is made.

The most common primitive constraint function is the ***At-point*** or ***Point Coincident Constraint***. If two *markers* on two *parts* k and l are compelled to remain coincident at all times irrespective of the orientation of their attached triad of axes, then the constraint function can be stated as:

$$C_{kl}=\left(R_k+r_k\right)-\left(R_l+r_l\right)=0 \qquad (1.21)$$

where R is the global position vector of the centre of mass of the part upon which a marker is defined and r is the local position vector of the marker from its centre of mass. Clearly, the global position vectors are function of the co-ordinates ξ^j, whereas the local position vectors are functions of q_k^i and need to be transformed to the former, using equation (1.19). Thus:

$$C_{kl}=\left\{\xi_k^j-\xi_l^j\right\}^T+\left\{\left[T\right]_k\xi_k^j-\left[T\right]_l\xi_l^j\right\}^T=0 \quad \text{for } j=1,3 \qquad (1.22)$$

This yields 3 constraint functions as indicated. Therefore, 3 degrees of freedom are removed. A ***spherical joint*** or a ***ball-in-socket joint*** are simply described by an at-point constraint.

Some constraint functions are related to orientation of *parts* with respect to each other, such as co-directing the axes of two parts to form a hinge. If the nominated co-directed axes for a ***hinge primitive constraint*** on markers k and l of two *parts* are q_k^3 and q_l^3, then:

$$q_k^3 \bullet q_l^1=0 \text{ and } q_k^3 \bullet q_l^2=0 \qquad (1.23)$$

where the dot product renders scalar constraint functions. Clearly, the co-ordinates q_k^i and q_l^i should be transformed to the global co-ordinates as before, thus an expression of the form $C_{kl} = [T]_k [T]_l \xi_k^j \xi_l^j = 0$ is obtained for both cases in (1.23), removing two degrees of freedom. The addition of the at-point and hinge primitive constraints at a location for markers k and l results in a ***revolute joint***. Therefore, a revolute joint introduces 5 constraints.

In a mechanical multi-body system *parts* are joined together by various joints or couplers (these relate motion of two *parts* such as rack and pinion). Once the appropriate constraint functions are determined, the appropriate reactions; $\sum_m \lambda_m \frac{\partial C_{kl}}{\partial \xi^j}$ are obtained. Now a set of equations of motion are found. These need to be solved simultaneously with the constraint functions themselves as previously described in section 1.2. Thus, the differential-algebraic equation set is:

$$\frac{d}{dt}\left(\frac{\partial K}{\partial \dot{\xi}^j}\right) + \frac{\partial U}{\partial \xi^j} + \sum_m \lambda_m \frac{\partial C_{kl}}{\partial \xi^j} = F_{a\xi^j} \quad \text{and} \quad C_{kl} = f(\xi^j) = 0 \qquad (1.24)$$

Rahnejat (1998) and Orlandea (1999, 2008) describe in detail the various methods of solution. However, a number of important points should be made since multi-body dynamic analysis codes are now readily available and increasingly used in industry and academe.

Firstly, in a dynamic analysis only suitably small changes in co-ordinates are permitted within a time marching integration method with small time steps δt. The solution is usually made by making substitutions: $\vartheta_k^j = \dot{\xi}_k^j$. Hence, the vector of unknowns to be determined is $\{\delta\vartheta_k^j, \delta\dot{\vartheta}_k^j, \delta\lambda_m\}^T$. Often, users of multi-body codes choose inappropriate time step size for their models' simulation. As a rough guideline δt is related to the rate of change of system variables (the required solution vector). Small time steps of few tenths of second suffice for large displacement rigid body dynamics, but not when impulsive loading or impact forces are involved. Impact durations are usually of the order of few tenths to several milli-seconds, requiring very small time steps. All contact dynamic problems usually require time steps of the order of micro-seconds. Secondly, time marching simulation studies are usually iterative, requiring convergence criteria set to be satisfied. Various chapters in this book describe choice of criteria and size of error tolerated for a sensible solution vector to be found. For detailed discussion of this point readers are referred to Rahnejat (1998). Finally, one should note that in practice *rigid* constraints do not exist and all real joints are subject to deformation under load. Only if the applied loads are insufficient, a rigid constraint may be assumed. Joints such as ball-in-socket are also subject to friction, which is ignored when they are considered as rigid idealised constraints. The same is true of some couplers,

such as assumed gearing constraint, where a common velocity marker on a meshing pair is assumed. Meshing pairs are subject to contact loads as a function of their lubricated separation and friction due to viscous shear of a lubricant film and potential asperity interactions (see, for example, the appendices in this chapter and chapters 15, 20 and 29). Furthermore, a common velocity *marker* may only be assumed at the pitch point of a teeth pair contact, whilst elsewhere during meshing slide-roll motion occurs.

Nevertheless, for particular types of analysis one may choose a combination of joints to either eliminate certain degrees of freedom or, for example, render a kinematic analysis (no degrees of freedom; mechanism follows a prescribed motion; note that a motion function introduces a constraint). Two other problems can occur with use of constraints in order to create a model, representative of a multi-body system. One is the use of what physically represents a practical joint in a closest manner. This can render an over-constrained multi-body model. Note that rigid constraints do not exist in practical mechanisms, but are mathematically convenient. The other problem is to introduce in a model constraint functions which replicate one another (***repeat constraints***). If such constraint functions are parts of a defined joint (as in commercial software) repeat constraints lead to redundant equations which are then automatically removed. The ensuing analysis would now be different to that intended or expected.

The method for representation of multi-body dynamics presented here is based on ***constrained Lagrangian dynamics***, where a system is defined in a reduced configuration space with respect to a global frame of reference. An alternative and older method was developed by Euler, now referred to as the ***Newton-Euler method***. This is based on direct application of Newton's second axiom, as in equation (1.1). It is, therefore, clear that all the forces acting on an element (*part*) of a system in $\sum_i F_i$ must be known *apriori*. The ingenious of Euler was to propose the use of free-body diagrams for constituent parts of a system, where reaction forces as in $F_{q^i} = -\frac{\partial U}{\partial q^i}$ can be specified to ensure the continuity of the system as a whole (figure 1.2). A series of equations (as in (1.1)) result for all parts of the system in the Euler frame of reference (previously described). It is clear that only the unconstrained degrees of freedom need to be modelled in this case, thus a smaller set of equations than those in constrained Lagrangian dynamics would result. This is the advantage of the Newton-Euler method. Its main disadvantage is that the omission of any reaction/restoring force can lead to an incorrect outcome. Furthermore, it is often difficult to visualise the degrees of freedom of a complex mechanism, prior knowledge of which is not required in the Lagrangian approach. Therefore, the Newton-Euler method demands from users a greater understanding of dynamics. All other methods developed since Lagrange and Euler are variations of the same with different interpretations or for manipulation of larger degrees of freedom systems, as a sparse matrix tableaux (Orlandea, 1999, 2008).

Although the use of constrained Lagrangian dynamics in multi-body software packages has made dynamics more accessible to the novice and uninitiated, certain considerations are essential and care is required in the development of models. Firstly, the approach becomes more useful with larger systems, and particularly inefficient with simpler systems (where Newton-Euler approach should be preferred). Secondly, it is necessary to determine the degrees of freedom of the eventually constructed model to ensure: (i)- the model is not over-constrained, (ii)- no repeat/redundant constraints exist and (iii)- the remaining degrees of freedom can be identified and verified. The ***Gruebler-Kutzbach expression*** can be used to ascertain the degrees of freedom of a system model:

$$nDOF = 6(n-1) - \sum_{m} C \qquad (1.25)$$

where n is the number of *parts* in a multi-body system including the ground (the assumed extraneous rigid environment), m is the number of constraint functions and C is the number of constraints introduced by each constraining function. For some standard mechanical joints, the number of constraints introduced are: spherical: 3, universal/hook: 4, revolute: 5, translational: 5 and cylindrical: 4. Each specified motion introduces a constraint, so do the couplers. Thus, systems which yield zero degrees of freedom with a or a number of specified motions are ***kinematic***. In such cases no solution to equations of motion is required (the underlying cause; forces, are of no concern). Thus, the solution is obtained by simultaneous solution of constraint functions, $C_{kl} = f(\xi^j) = 0$, which includes the specified motion(s).

For ***static analysis***, let: $\dot{\vartheta}_k^j = 0$ in equations (1.24). The solution vector $\{\vartheta_k^j, 0, \lambda_j\}^T$ corresponds to the equilibrium position, where $\sum_j F_j = 0$. If the solution vector has a unique solution, then static condition is obtained. A multitude of such solutions corresponds to a ***quasi-static analysis***.

1.5- Engine as a Multi-body System

Perhaps the simplest multi-body model of an engine would be that of a single cylinder kinematic model. Such a model would be useful as a visualisation tool or simply to identify constraint functions required for a subsequent dynamics analysis. Figure 1.1 shows such a model. The *parts* in the engine are considered to be: flywheel, crankshaft, piston and connecting rod. The ground (the boundary of the system) is considered to be the cylinder block and beyond. The parts are numbered as $k = 1,2,3$ and 99 respectively as shown in the figure. Therefore, in the Gruebler-Kutzbach expression $n = 5$. The mechanical joints are so chosen in order to avoid repeat or redundant constraint functions. For example, the cylindrical joint, representing the big end bearing between the connecting rod and the crank-pin allows translation of crankshaft relative to the connecting rod. However, this is constrained by

the revolute joint between the crankshaft and the ground. The universal joint at the position of the small end bearing allows the articulation of the connecting rod relative to the piston. However, it also enables the piston to tilt back and forth (in and out of the plane of paper), which is constrained by the cylindrical joint between the piston and the ground. Thus, there are no repeat/redundant constraints. In practice, the motion of the crankshaft is specified by the combustion gas force as $C_{kl} = C_{199} = 2\pi Nt$, N being the rotational speed in rev/sec. Using the Gruebler-Kutzbach expression:

$nDof = 6(5-1) - \sum(1X\ \underbrace{6}_{Fxd} + 1X\ \underbrace{5}_{\mathrm{Rev}} + 2X\ \underbrace{4}_{Cyl} + 1X\ \underbrace{4}_{Uni} + 1X\ \underbrace{1}_{Mot}) = 24 - 24 = 0$, thus a kinematic model results, which follows the specified motion.

Kinematic models, using other combination of constraints may also be found. For example, an alternative choice is a translational joint between the piston and the ground, a revolute joint between the piston and the connecting rod, representing the wrist-pin bearing, an in-line joint between the connecting rod crankshaft. The flywheel is considered fixed to the crankshaft. and the crankshaft has a revolute joint to the ground with the same specified motion as before. Thus: $nDof = 6(4-1) - \sum(2X\ \underbrace{5}_{\mathrm{Rev}} + 1X\ \underbrace{5}_{Tra} + 1X\ \underbrace{2}_{Inl} + 1X\ \underbrace{1}_{Mot}) = 18 - 18 = 0$.

Note that the ***in-line primitive constraint*** introduces 2 constraint functions as:

$$C_{kl} = \left\{\left(R_k + r_k\right) - \left(R_l + r_l\right)\right\} \bullet q^l{}_{|l=1,2} = \left\{\left\{\xi_k^j - \xi_l^j\right\}^T + \left\{[T]_k \xi_k^j - [T]_l \xi_l^j\right\}^T\right\} \bullet \left\{[T]_l \xi^j_{l|l=1,2}\right\}^T = 0$$

If k represents a marker on the crank/flywheel assembly and l the coincident marker on the connecting rod, then k can translate with respect to l with all its rotational freedoms intact. However, the translational motion is constrained by the revolute joint to the ground.

The motion constraint is in fact governed by the combustion process, with an initial condition, usually determined by the starter motor characteristics. Therefore, one can achieve a very basic dynamics model simply by removing the specified motion constraint and apply the gas force instead to the piston. A one degree of freedom system results, which couples the translational motion of the piston to rotation of the flywheel-crank assembly. Mass and inertial properties of the parts in the system should be specified. Choice of constraint functions in the assembly of parts can now be quite important, depending on the intended analysis.

For basic tribological studies, suitable constraint functions must be chosen to allow motions that are constrained in the previous examples. For instance, piston has secondary motions as described in chapters 8, 10-15, involving piston lateral motion within the confine of its clearance with the cylinder liner or bore, as well as tilting motion about the axis of the wrist-pin bearing. Therefore, it is clear that choice of a translation joint between the piston and

the ground (the engine block) prohibits these motions. The same is true of an inline primitive constraint at the position of the big end bearing, constraining the lateral motions of crank-pin journal centre with respect to the bushing/sleeve fitted onto the connecting rod. The inline primitive constraint can be replaced by a ***planar constraint***, which can best be described as a hockey puck sliding on ice. If the puck is regarded as *part* k and the ice surface as *part* l, then this joint primitive allows rotation with respect to their common orthogonal axis with no translation, whilst rotation about other axes are also constrained, so that contact is maintained at all times. These lateral axes of part k can translate with those of part l allowing sliding motion of the puck. Thus, 3 constraint function are introduced. If k represents the crankshaft and l the connecting rod, then: $C_{kl} = \{(R_k + r_k) - (R_l + r_l)\} \bullet q_l^3 = 0$ and $q_k^3 \bullet q_l^i\big|_{i\in 1,2} = 0$, which introduces 3 constraints, which can be transformed in terms of the co-ordinates ξ_l^j, ξ_k^j. To avoid repeat constraints, the revolute joint between crank/flywheel assembly is replaced by a cylindrical joint as the planar joint already inhibits motion along the crank axis. The revolute joint between the connecting rod and the piston is also replaced by a spherical joint as the rotations of the connecting rod other than that about the wrist-pin axis are already constrained by the planar constraint functions. The rotation of the crankshaft is determined by the combustion curve (gas force). Hence, the motion constraint remains, this time with an applied gas force on the piston. A two degrees-of-freedom dynamic model results which correspond to the lateral motions of the crank/flywheel assembly relative to the connecting rod (the motion of the crank-pin journal relative to the bushing/sleeve). To restrict these (restraints), journal bearing forces should be used, similar to those described in chapters 18-20 as functions of the eccentricity ratio. Hence:

$$nDof = 6(4-1) - \sum(1X\underbrace{4}_{Cyl} + 1X\underbrace{5}_{Tra} + 1X\underbrace{3}_{Sph} + 1X\underbrace{3}_{Pla} + 1X\underbrace{1}_{Mot}) = 18 - 16 = 2$$

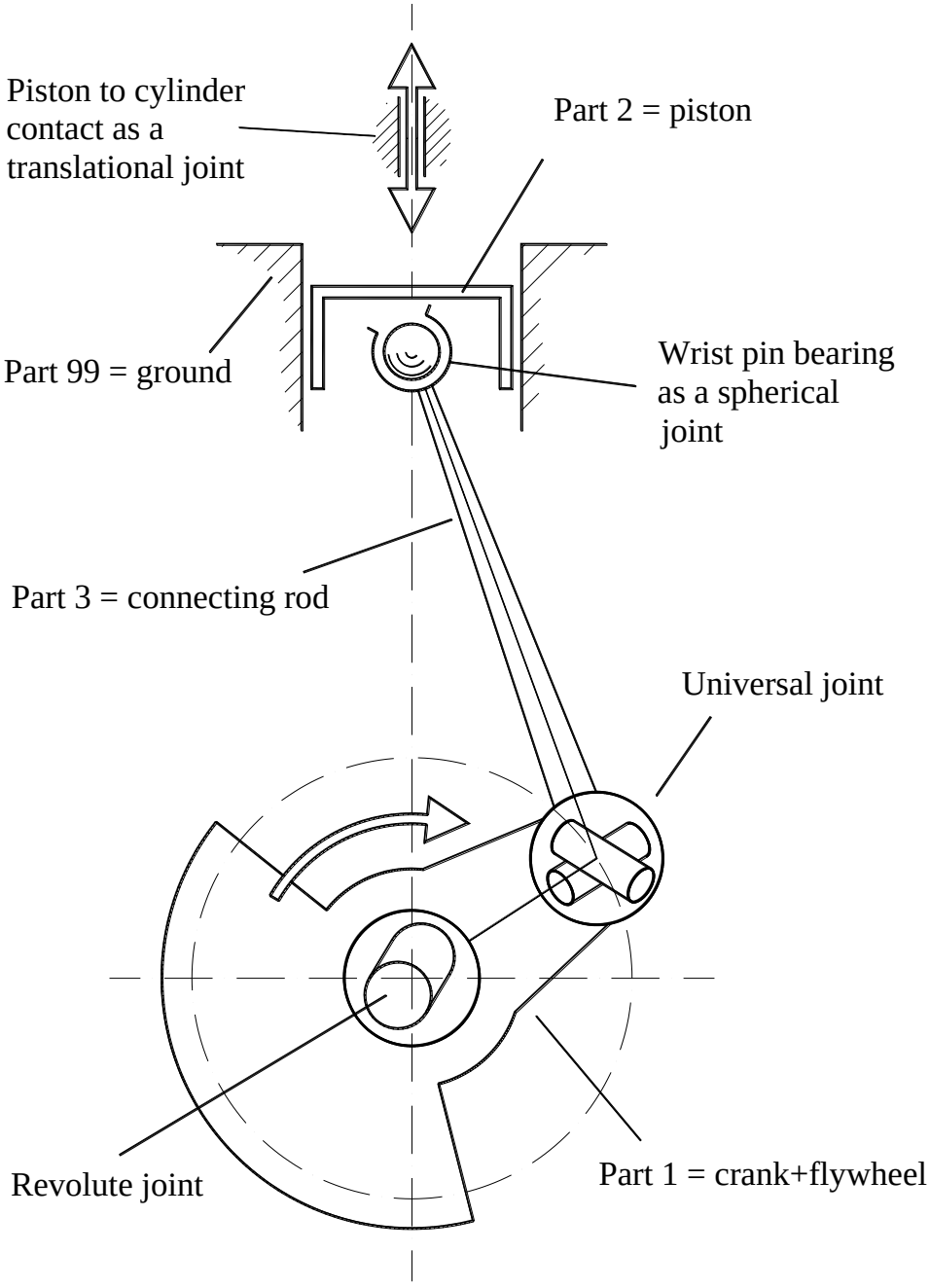

Figure 1.1: A kinematic model for a single cylinder engine

Therefore, multi-body models with suitable constraints can be developed to enable description of load bearing conjunctions, where important tribological contributions to system dynamics can be included in the analysis.

Most multi-body dynamic analyses, however, were initially performed for low frequency phenomena such as suspension analysis, ride comfort and vehicle handling responses. Rahnejat (1998) provides some basic examples. Larger detailed vehicle models are commonly used in industry as a part of vehicle development programmes. Representative literature include a series of

papers by Blundell (1999), Hegazy *et al* (2000) and Hussain *et al* (2007), which include tyre forces, aerodynamic forces and complex manoeuvres (see also chapter 23, using the Newton-Euler approach).

Inclusion of component flexibility became possible later with integration of finite element techniques and multi-body methods through mode reduction and selection techniques such as component mode synthesis. This enabled representative analysis of systems as they are subject to deformation loads. A good example is the inclusion of anti-roll bars in vehicle models, where its structural compliance resists vehicle roll during cornering manoeuvres. Another example is the inclusion of structural resistive suspension elements such as leading or trailing arms, which restrict vehicle dive in braking or squat under sudden acceleration (see Azman *et al*, 2007). These phenomena are still low to medium frequency events, dominated by large displacement dynamics (that of the sprung or unsprung masses).

In recent years multi-body dynamics approach has been used in conjunction with tribological studies (for example see Boysal and Rahnejat, 1997). Some detailed models, including component flexibility are presented by Kushwaha *et al* (2002) and Perera *et al* (2007) for engine and drivetrain dynamics with experimental validation. It is important to briefly describe the increasing need for inclusion of component flexibility in multi-body dynamics models, as well as different methods which can be employed to achieve this.

1.6- Elasto-multi-body dynamics analysis

Component flexibility plays an important role in dynamics of real systems. Its role has become more pronounced in recent years with increasing use of lighter components in an effort to reduce mechanical losses (mainly due to out-of-balances) and thus enhance fuel efficiency. However, lighter components, often made of materials of lower elastic modulus or with increasing use of hollow components are subject to elastic deformations and vibration. In the case of engines and power trains a plethora of noise and vibration concerns have emerged in the past two decades due to component flexibility as well as increased output power (for example higher torques in diesel engines). Some of these noise and vibration problems are discussed in this book, such as transmission rattle (see chapters 21, 26-29 and also the appendix in this chapter) and driveline clonk (see chapter 21 and 30). There are many other such NVH concerns, such as vehicle body boom (see chapter 21), engine roughness (Rahnejat, 1998) and clutch in-cycle vibration or whoop (Kushwaha *et al*, 2002).

Rahnejat (1998) describes some of the basic modelling approaches to include component flexibility. These include Transfer Matrix Method (TMM) and Dynamic Stiffness Matrix Method. Other advanced methods are described by Shabana (2005) and Nikravesh (2008). Here a number of basic approaches are highlighted.

A simple approach to represent flexibility is by ***Eulerian beams***. Compliance functions relate 6 restrained (elastic) degrees of freedom motion of one end of the beam (e.g. $q^i \in x, y, z, \theta, \phi, \psi$) with respect to the forces applied at the other (e.g. $F_{aq^i} \in F_x, F_y, F_z, T_x, T_y, T_z$) (see figure 1.2). The mass of the flexible part is discretised into two masses concentrated at the either ends of the beam. Therefore, these masses act as *parts* and would require inertial properties. In multi-body terminology they are referred to as dummy parts, because often they are a specific component of a mechanical system. For example, crankshaft flexibility may be represented by crank-pins as Eulerian beams and crank-webs as the point masses, generally referred to as concentrated inertial elements. The beams act as restraining elements which introduce forces between the dummy parts or in the case of the crankshaft between the successive crank-webs as:

$$\{F_{aq^i}\}^T = \begin{bmatrix} \frac{EA}{L} & 0 & 0 & 0 & 0 & 0 \\ 0 & \frac{12EI_{q^3}}{L^3} & 0 & 0 & 0 & \frac{-6EI_{q^3}}{L^2} \\ 0 & 0 & \frac{12EI_{q^2}}{L^3} & 0 & \frac{6EI_{q^2}}{L^2} & 0 \\ 0 & 0 & 0 & \frac{GI_{q^1}}{L} & 0 & 0 \\ 0 & 0 & \frac{6EI_{q^2}}{L^2} & 0 & \frac{4EI_{q^2}}{L} & 0 \\ 0 & \frac{-6EI_{q^3}}{L^2} & 0 & 0 & 0 & \frac{4EI_{q^3}}{L} \end{bmatrix} \{\delta q^i\}^T - [D]\{\delta \dot{q}^i\}^T \quad (1.26)$$

where, these restraining/resistive forces are treated as applied forces. Note the longitudinal axis of the beam is designated as q^1 in the stiffness matrix above. $[D]$ is the damping matrix, elements of which are usually quite difficult to specify. A simple approach is to specify its elements as a percentage of the stiffness matrix (usually around 1% for lightly damped power train components). The restraining forces are then transformed to the co-ordinates ξ^j, using equation (1.19) for $\{\delta q^i\}$ for $i \in 1,2,3$ and for $i \in 4,5,6$ the Euler transformation matrix $[T^*]$ is used, as described in section 1.4.1. This is the basis of ***transfer matrix method*** (TMM) (see Rahnejat, 1998).

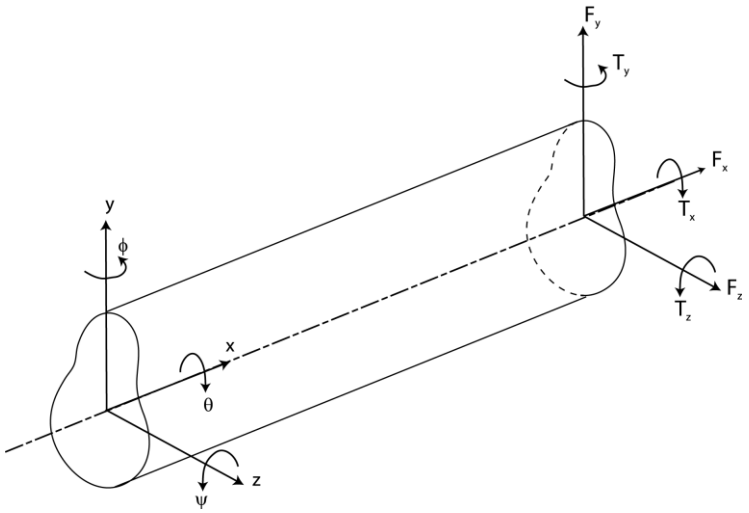

Figure 1.2: An Eulerian beam

It is clear that if a crank-pin is considered as a single beam element, then many of its torsional-bending modes would be ignored. Thus, flexible parts may have to be discretised into more than a single beam interspersed with dummy parts between successive beams. The more flexible the structure or larger the deformation energy, a greater number of discretisations would be required (more mode shapes). This approach leads to ever smaller beams or in fact any regions, where certain stress-strain (load-deflection) relationships may be assumed. These regions are usually referred to as finite elements. Therefore, finite element analysis provides the right approach in determining the modal behaviour of flexible structures.

Unlike the bodies which are considered to be rigid, the elastic bodies undergo deformation whilst in motion. Therefore, a flexible body may itself be regarded as a constrained configuration space described by a set of co-ordinates, referred to as ***elastic co-ordinates***. Its inertial behaviour remains the same as before; described by the global position vector of a reference point on it (e.g. centre of mass) with respect to the global frame of reference as already described. Therefore, the elastic deformation of the body is described by the elastic co-ordinates of its many points with respect to the local part frame of reference at the nominated reference point and through transformation to the global frame of reference.

$$R_k^p = R_k^0 + u_k^p = R_k^0 + f(r_k^B + \delta_k^p) \qquad (1.27)$$

where, the point *B* is an *initial* position of a point *P* prior to its deformation δ_k^p in a small time step δt. Clearly, the function $f(r_k^B + \delta_k^p)$ is a shape function, referred to as a mode shape or eigen-vector which should be determined. One general way of including this function in (1.27) is through finite element analysis.

As already described in FEA a continuous flexible body can be represented by a collection of interconnected elemental regions with specified constitutive (stress-strain) relations. The stiffness and mass matrices for the these elements can be obtained using assumed shape functions. This involves evaluation of mass and stiffness matrices to represent the elemental behaviour for given assumed shape functions as:

$$\left[m_\xi\right] = \left[T\right]^T \left[m_q\right]\left[T\right] \text{ and } \left[k_\xi\right] = \left[T\right]^T \left[k_q\right]\left[T\right] \tag{1.28}$$

In the same manner the corresponding resistive forces associated with points *P* (nodes in the finite elements), F_{aq^i} can be transformed to the global co-ordinates: $F_{\xi^j} = \left[T\right]^T F_{aq^i}$.

For Eulerian beams the localised stiffness martrix is given in (1.26) and the mass matrix in (1.28), $\left[m_\xi\right]$ is termed the *consistent mass matrix* as it is obtained for the same shape functions assumed for the calculation of the stiffness matrix. Now equations of motion for a flexible part can be written, using the same approach as before. Furthermore, there would be no need to concentrate the mass of a flexible member in certain locations.

However, with many finite elements a very large degree of freedom can result, corresponding to many mode shapes ϕ_i, all of which would contribute to δ_k^p as a linear combination in the local frame of reference q^k:

$$\delta_k^p = \sum_{i=1}^{n} \phi_i q^i = \Phi_k q^k \tag{1.29}$$

where n is the number of mode shapes and Φ_k is the modal matrix for the body *k*. Equation (1.29) effectively transforms a larger set of physical coordinates δ_k^p to a smaller set of modal coordinates q^k. Depending on component geometry and physical state and nature of loading, the modal matrix can be very large indeed. Hollow thin walled tubes, for example (e.g. driveshaft tubes), have many coupled torsional-bending modes (see chapter 30). These are usually represented by combination of circumferential and axial waves on the tubes, such as those shown in chapter 30. Such structures are said to have a high modal density. On the other hand, short and stubby solid structures made of materials of high elastic modulus can potentially only undergo rigid body motions, even when subjected to moderately high loads, such as machine tool spindles. Depending on loading and purpose of investigation a ***reduced order model*** may suffice, by considering certain modal responses to be constrained. A reduced order model can be achieved by solving only for $m < n$ mode shapes, because of the *modal superposition* approach in (1.29). Therefore, mode shapes should be selected in a manner

that results in a good approximation for a pre-determined frequency band of interest.

The basic technique used is ***component mode synthesis*** (Craig, 1995), where the physical co-ordinates δ_k^p for a component *k* is divided into boundary components which are regarded as not being subject to modal superposition (*elastically* constrained, dependent DOFs), δ_{dk}^p and those which are subject to deformation (independent DOFs), δ_{ik}^p. Now if $\delta_{dk}^p = 0$ because of the imposed constraints, then:

$$[m_{ik}]\{\ddot{\delta}_{ik}^P\} + [k_{ik}]\{\dot{\delta}_{ik}^P\} = \{f_{ik}\} \qquad (1.30)$$

Combining this equation with (1.29) enables substitution for physical co-ordinates δ_{ik}^p with the reduced number of modal co-ordinates ϕ, using FEA. The detailed procedure is described in Gnanakumarr *et al* (2005).

With component flexibility included in a multi-body model other important features to be incorporated are usually contact/impact and frictional forces. This means that realistic models for all forms of machines and mechanisms can be constructed. Such models incorporate various physical characteristics; inertial, elasticity, tribological, etc; thus may be regarded as multi-physics. The also comprise interactions at the various scales; large displacements, vibration and micro-scale tribology; thus multi-scale. The most appropriate way to demonstrate such an approach is through some examples. In the appendices to this chapter two of Loughborough's researchers describe analysis of some of the most pertinent current concerns in the automobile industry.

1.7- Appendix A1: Multi-physics analysis for investigation of manual transmission gear rattle: Drive/creep rattle

M. De la Cruz, Wolfson School of Mechanical & Manufacturing Engineering, Loughborough University, Loughborough, UK

Nomenclature:

b	Minor semi-half-width of contact
C	Backlash
C_p	Specific heat capacity
c	Clearance between loose wheel and retaining shaft
E^*	Effective elastic modulus (see chapter 4)
F_b	Boundary friction
F_v	Viscous friction
$F_{fwi,j}$	Flank friction per teeth pair
F_{pi}	Petrof friction of loose wheels

h Film thickness
I_2 Inertia of 2nd gear
I_i Inertia of loose wheels
I_{os} Inertia of output shaft
I_7 Inertia of reverse pinion
k_t Thermal conductivity of transmission fluid
l Contact length
l_{brg} Gear blank width
m Equivalent mass
N Relative rotation of loose wheel and retaining shaft in rev/s
p Pressure
Q_s Side leakage flow
R_{brgi} Radius of supporting shaft of loose wheel
R_{bpi} Base radius of pinion
R_{bwi} Base radius of wheel
$r_{xi,j}$ Equivalent radius of a teeth pair in x-z plane (see chapter 4)
T_{D2} Resistive torque of differential referred to 2nd gear
u Speed of entraining motion (average speed of a meshing teeth pair)
Δu Sliding velocity (relative surface speed of a meshing teeth pair)
u_{brg} Speed of entraining motion in the loose wheel-to-shaft conjunction
v_e Coefficient of thermal expansion
v_p Velocity of approach of contacting/impacting gear teeth pair
v_x Surface velocity in the x-direction
W_{brg} Hydrodynamic load in the loose wheel-to-shaft conjunction
$W_{i,k}$ Contact load per teeth pair
α Pressure-viscosity coefficient of the transmission fluid
α^* Temperature dependant pressure-viscosity coefficient
δ Contact elastic deflection
ε Eccentricity ratio
θ Temperature
φ_i Rotational displacement of wheel
φ_{os} Angular displacement of output shaft
φ_p Rotational displacement of pinion
η Effective dynamic viscosity at contact temperature
η_o Dynamic viscosity at bulk oil temperature and atmospheric pressure
ρ Density
ψ Attitude angle in the wheel-to-shaft conjunction

(a)- Mathematical Formulation

Rahnejat, H., "An introduction to multi-physics multi-scale approach", in Rahnejat, H (Ed.), Tribology and dynamics of engine and power train, Woodhead Publishing, Cambridge, UK, 2010, ISBN: 978-1-84569-361-9

Gear teeth impacts (***rattle***) are induced due to oscillations of loose (unselected) gears within the confine of their clearances. These oscillations are caused by torsional fluctuations of the transmission input shaft caused by combination of engine inertial imbalance and combustion loading (referred to as ***engine order vibrations***, see Rahnejat, 1998). These vibrations are particularly present in diesel engines output torque. Due to various driving conditions, different types of rattle have been defined; idle, drive, creep and over-run rattles (see chapters 21, 23-30). It is noteworthy, however, that rattle only originates within the unselected gear pairs. The distinction described above only changes the gearbox's input shaft excitations and the contribution of a given engaged gear to its counterparts. Figure A1-1 shows a diagrammatic representation of a 6 speed forward plus reverse manual gearbox used in this analysis (also see chapter 26).

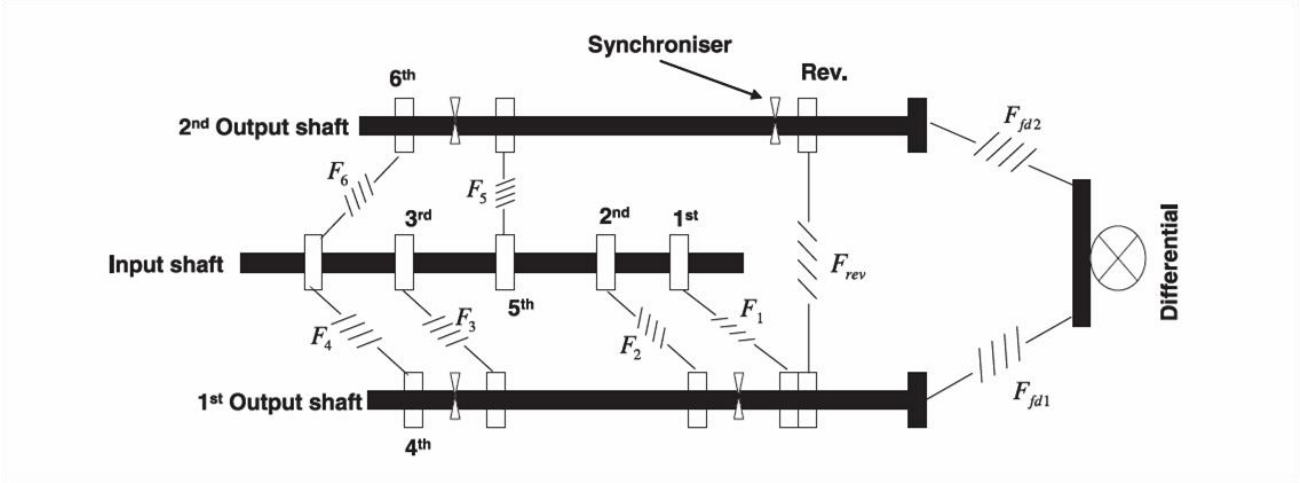

Figure A1.1: Front wheel drive, 6 speed + reverse gearbox under investigation

In the multi-physics approach described in this chapter, the model comprises inertial dynamics and impact/contact tribological characteristics. There are a number of lubricated conjunctions, shown in figure A1.2.

Rahnejat, H., "An introduction to multi-physics multi-scale approach", in Rahnejat, H (Ed.), Tribology and dynamics of engine and power train, Woodhead Publishing, Cambridge, UK, 2010, ISBN: 978-1-84569-361-9

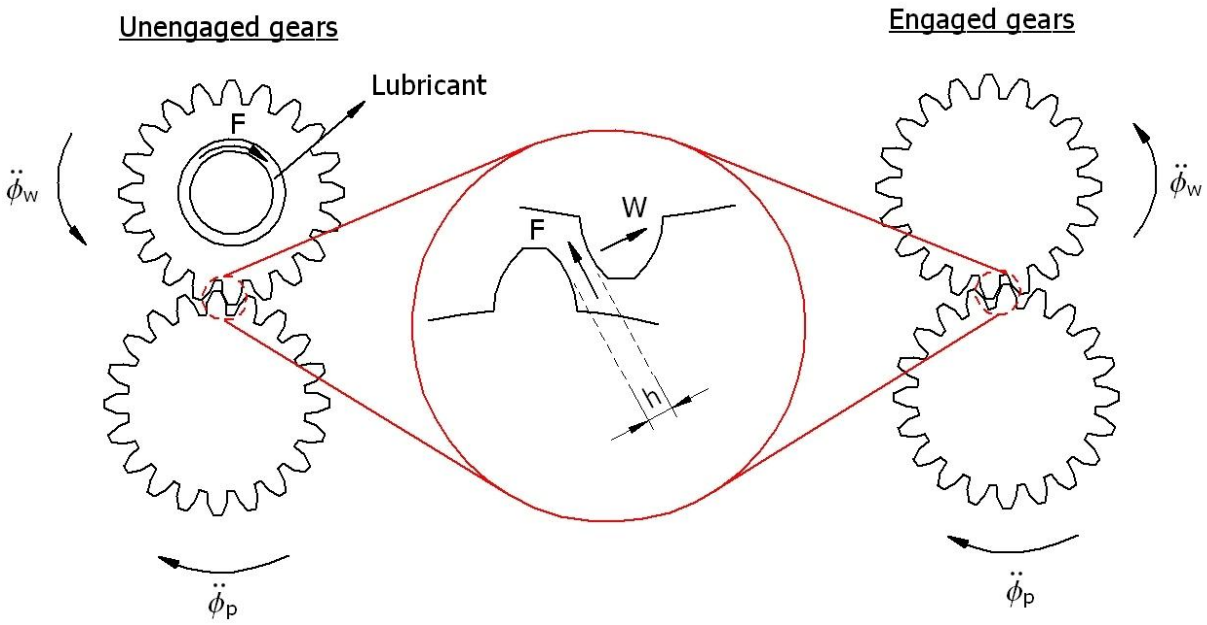

Figure A1.2: Forcing elements in conjunctions of engaged and unengaged gear pairs

For the loose rattling gear wheels, the regime of lubrication is assumed to be hydrodynamic (see chapter 5). This assumption is supported by the low loads, W and a relatively large film thickness, h. In the case of engaged gear pair, this assumption is no longer true as moderate to high loads lead to elastohydrodynamic regime of lubrication (***EHL***) (see chapter 6). These assumptions have been verified through use of a lubrication chart, such as that presented in Gohar and Rahnejat (2008). Typically, EHL conjunctions, have film thicknesses in the sub-micrometer region.

Grubin (1949) provided the original analytical solution to the EHL problem. Equation A1.1 presents Grubin's expression for film thickness:

$$\frac{h}{r_x} = 2.076\left(\frac{\alpha\eta u}{r_x}\right)^{8/11}\left(\frac{E^* l r_x}{W}\right)^{1/11} \qquad \text{(A1.1)}$$

The contact load can be obtained through Hertzian analysis for an elastic line contact as:

$$W \approx \left[\frac{\pi l E^*}{2\left[\ln\left(\frac{2l}{b}+\frac{1}{2}\right)\right]}\right]\delta \qquad \text{(A1.2)}$$

where, under a totally elastic impact, the deflection is found as (Gohar and Rahnejat, 2008):

$$\delta = \left[\frac{2\left(\ln\left(\frac{2l}{b} + \frac{1}{2} \right) m v_p^2 \right)}{\pi l E^*} \right]^{1/2} \quad \text{(A1.3)}$$

With the aid of kinematics and Hertzian contact mechanics, all the parameters needed in equations (A1.3) are found (De la Cruz *et al,* 2008*)*.

Friction for thin EHL films in gear pair contacts is due to a combination of viscous shear and boundary interactions, thus:

$$F = F_b + F_v \quad \text{(A1.4)}$$

This is rather involved and readers should refer to Greenwood and Tripp (1967) model (see also chapter 3).

Hydrodynamic reactions in loose gear teeth pairs are represented by the analytical relationship (Gohar and Rahnejat, 2008):

$$W = \frac{2bu\eta r_x}{h} - \frac{3\pi b\eta}{\sqrt{2}} \left(\frac{r_x}{h} \right)^{3/2} \frac{\partial h}{\partial t} \quad \text{(A1.5)}$$

The expressions are also based on contact geometry and operating conditions. A very important parameter is the squeeze film velocity in approach and separation of gear teeth pairs (see chapter 5); $\frac{\partial h}{\partial t}$. A negative value corresponds to the approach of the contacting solids (increasing the contact load in (A1.5)). When a positive value is encountered, this is set to zero, i.e. entraining motion only, as the lubricant cannot sustain a tensile force.

The film thickness value for use in equation (A1.5) is obtained as a function of gear pair dynamics (Tangasawi *et al*, 2007):

$$h = C - \left| R_{bwi}\varphi_i - R_{bpi}\varphi_{pi} \right| \quad \text{(A1.6)}$$

As can be seen in figure A1.2, there are two distinct conjunctions in loose gear pairs. One conjunction corresponds to the impact/contact zones of gear teeth pairs, in which flank friction is generated due to viscous shear under hydrodynamic condition. A number of teeth pairs are usually in simultaneous action. The flank friction in each pair is a function of the contact sliding velocity, thus (Gohar, 2001):

$$F_{fw} = \begin{cases} \dfrac{l\pi\eta\Delta u}{\sqrt{2h}}\sqrt{r_x}, & \Delta u \geq 0, \\ \dfrac{-l\pi\eta\Delta u}{\sqrt{2h}}\sqrt{r_x}, & \Delta u < 0, \end{cases} \qquad \text{(A1.7)}$$

The other conjunction is the conforming contact between the output shaft supporting the loose wheel and the wheels inner (bore) surface. This contact may be approximated by a journal bearing with no eccentricity. The viscous friction in this conjunction is given as (Gohar and Rahnejat, 2008):

$$F_P = \frac{c\varepsilon W_{brg}}{2R_{brg}}\sin\psi + \frac{2\pi\eta u_{brg} R_{brg} l_{brg}}{c\left(1-\varepsilon^2\right)^{1/2}} \qquad \text{(A1.8)}$$

where $\varepsilon \approx 0$, thus: $F_P = \dfrac{2\pi\eta u_{brg} R_{brg} l_{brg}}{c}$

Having stated all the required forcing functions, based on the tribological contacts, the dynamics of the problem can now be introduced. This multi-body system is solved using equations of motion following the Newton-Euler approach. Hence, for the 7 degrees of freedom model presented in figure A1.1, the equations of motion can be divided into three groups:

For the engaged pinion-wheel pair (in this case the 2nd gear):

$$(I_2 + I_{os})\ddot{\varphi}_2 = \sum_{k=1,n'} W_{2,k} R_{bw2} - \sum_{i=1,3,4,7} \sum_{j=1,n} F_{i,j} r_{xi,j} - \sum_{k=1,n'} F_{2,k} r_{x2,k} - T_{D2} \qquad \text{(A1.9)}$$

For the loose unselected pinion-wheel pairs $i \in 3-6$:

$$I_i \ddot{\varphi}_i = \sum_{j=1,n'} W_{i,j} R_{bwi} - \sum_{j=1,n'} F_{i,j} r_{xi,j} - F_{pi} R_{brgi} \qquad \text{(A1.10)}$$

Finally, for the reverse pinion-wheel pair (loose wheel on the 2nd transmission output shaft, meshing with the reverse pinion mounted on the 1st output shaft):

$$I_7 \ddot{\varphi}_7 = \sum_{k=1,m'} W_{7,k} R_{bw7} - \sum_{k=1,m'} F_{7,k} r_{x7,k} - F_{p7} R_{brg7} \qquad \text{(A1.11)}$$

Under the EHL regime of lubrication, lubricant viscosity is dependent upon both the generated conjunctional pressures and temperature. Pressure causes a rise in viscosity and responsible lubricants almost incompressible behaviour (chapters 5 and 6). Also, due to the viscous shear in the contact temperature rises, which in turn reduces the lubricant viscosity (see chapter 5) In moderate to highly loaded concentrated contacts the conditions are referred to as ***thermo-elastohydrodynamics*** (see chapter 6). Thus, together

with the dynamics, the model is multi-physics, multi-level approach, dealing with variables from sub-micrometers (film thickness) to those of large displacements. For very small micro-electromechanical gear pairs (MEMS), the physics of conjunctions are in nano-scale (see Gohar and Rahnejat, 2008 and chapters 3 and 32).

Thermal effects must be accommodated in two major conjunctions, flank interactions and those of loose wheels-to-the retaining shaft. When dealing with heat generation in contacting flank pairs, the energy equation can be solved analytically (see chapter 5). The energy equation is:

$$\underbrace{v_e v_x \theta \left(\frac{\partial p}{\partial x}\right)}_{\text{compressive heating}} + \underbrace{\eta \left(\frac{\partial v_x}{\partial z}\right)^2}_{\text{viscous heating}} = \underbrace{\rho v_x C_p \left(\frac{\partial \theta}{\partial x}\right)}_{\text{convection cooling}} - \underbrace{k_c \left(\frac{\partial^2 \theta}{\partial z^2}\right)}_{\text{conduction cooling}} \qquad \text{(A1.12)}$$

For thin elastohydrodynamic films heat generation within the contact region is carried away by conduction through the contiguous surfaces. Thus, the convection cooling term may be ignored. Also, the compressive heating term is small compared with shear heating, particularly within the flat reion of the EHL film, thus an analytic solution is possible, where the temperature rise in the flat oil film is found as (Gohar and Rahnejat, 2008):

$$\Delta\theta = \frac{2\eta \Delta u^2}{k_t} \qquad \text{(A1.13)}$$

Under hydrodynamic conditions, relatively thicker films in the teeth flank conjunctions promote convection cooling and compressive heating can be ignored due to low pressures, thus:

$$\Delta\theta = \frac{8b\eta \Delta u}{h^2 \rho C_p} \qquad \text{(A1.14)}$$

For the conforming contact between the loose wheels and their retaining shafts, an analytic solution similar to that for a journal bearing may be used (see chapter 8 and Gohar and Rahnejat, 2008). Thus:

$$\Delta\theta = \left(\frac{2K_1 W_{brg}}{\rho C_p R_{brg} l_{brg}}\right)\left(\frac{\mu^*}{Q_s^*}\right) \qquad \text{(A1.15)}$$

where: $Q_s^* = \frac{Q_s}{\pi N l R c}$, $\mu^* = \frac{\mu R}{c}$ and $K_1 = \frac{k_1}{\rho c_p}$, where $k_1 < 1$ indicates that not all the heat is carried away by convection.

With $\Delta\theta$ obtained for each conjunction and the inlet bulk oil temperature known (that of engine operating condition), the effective viscosity of the

lubricant in each conjunction can be evaluated using Houpert (1985) equation. This is given in chapter 5. Thus, an iterative procedure is used which includes tribology, thermal effects and system dynamics (De la Cruz *et al*, 2009a).

(b)- Results and Discussion

Figure A1.3 shows the predictions for partial loading creep rattle condition at the engine idling speed of 830 engine RPM with 2nd gear engaged. Two different cases are presented; one for low and the other for high bulk oil temperature. Previous studies have indicated that temperature plays a key role in transmission rattle (see Tangasawi *et al*, 2007 and chapter 26). It is suggested that at higher temperatures loose gear pairs are more prone to rattle due to reduction in resistive (drag) torque. It has also been shown that at some *ideal temperature values* gear rattle is attenuated. It may be surmised that lubricant viscosity variation in different conjunctions, described above, may be the cause of this. However, this variation is different for each single gear pair and hence a unique solution may be difficult to find.

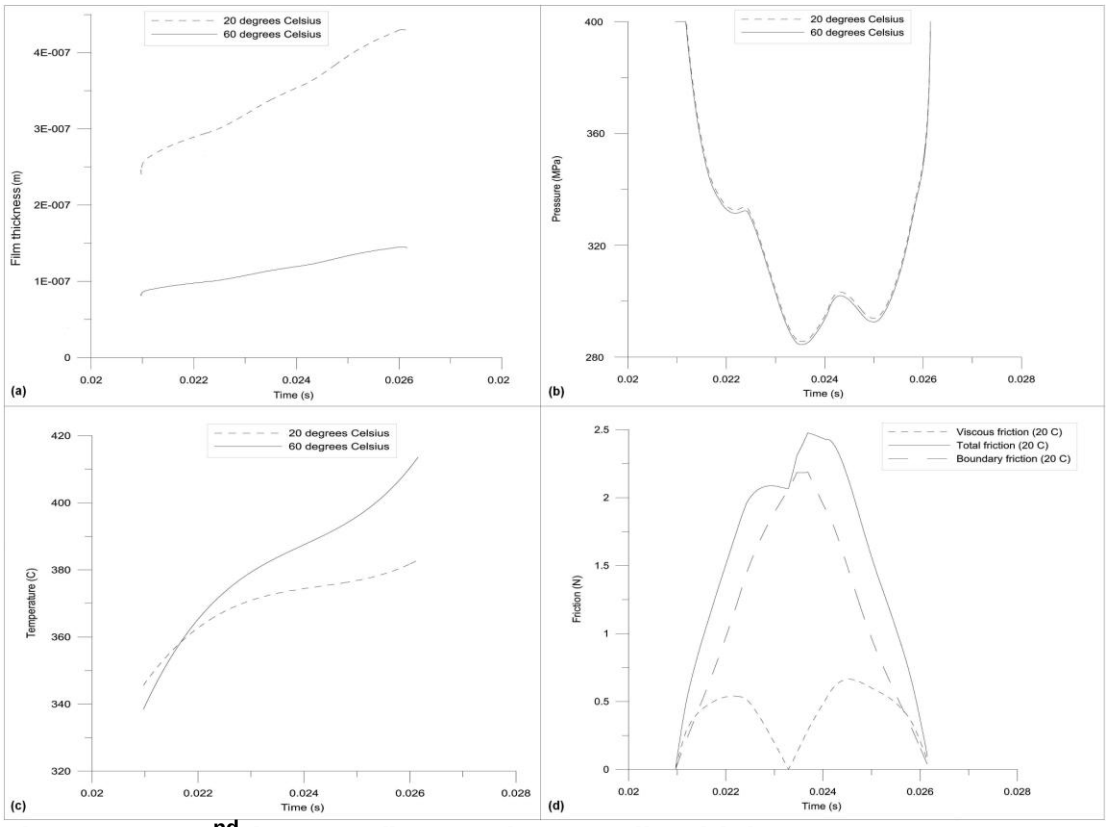

Figure A1.3: 2nd (engaged) gear plots for film thickness, mean pressure, friction and temperature change in a meshing cycle for a gear teeth pair

The result in figure A1.3 relate to one meshing cycle, comprising simultaneous interactions of 2-3 gear teeth pairs of the selected 2nd gear pair. The variations are for one set of teeth in order to demonstrate the effect of temperature, often ignored in all such analyses. As expected, due to EHL conditions the film thickness in general is rather insensitive to load, but

profoundly sensitive to contact temperature and geometry. This affects the flank friction and thus the torque transmitted to the loose gear pairs, which themselves are affected by temperature as well.

The changes as the result of meshing conditions in the engaged gear pair, together with engine order vibration transmitted to the loose unselected gear pairs induce transmission creep rattle in the case studied here. Further analysis of loose gear results, typically by fast Fourier analysis of their dynamic behaviour sheds light on their rattle behaviour. De la Cruz *et al* (2009b) used an ***impulsion ratio*** I_m, to define rattle conditions:

$$I_m = \frac{T_{drive}}{T_{drag}} \propto C \frac{C_{pet}\eta_f}{h\eta_{pet}} \qquad \text{(A1.16)}$$

This attempts to predict conditions that induce propensity to rattle. The ratio takes into account the inertial torque, inducing motion (due to impact forces of simultaneous meshing pairs) and the resistive or drag torque (because of frictional losses). A ratio of unity leads to uniform motion (no acceleration), whilst values exceeding unity indicate impulsive action and those below unity correspond to decaying oscillations.

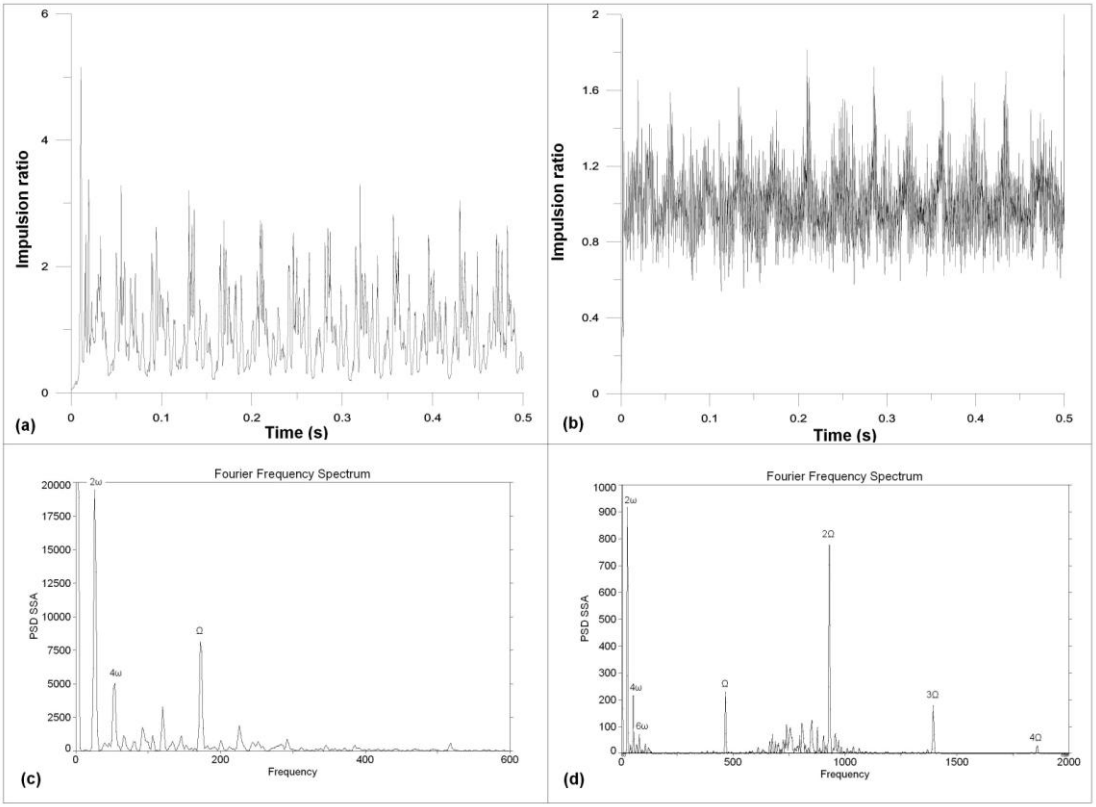

Figure 4 – Impulsion ratio time histories and FFT spectra for high (1st) and low inertia (5th) gears. (a) and (c) refer to 1st gear and (b) and (d) to 5th gear

It is noted that at a given temperature, high inertia gears show a lower energy content in their frequency spectrum, suggesting that rattle could be more noticeable in the low inertia gears. Even though the values of the impulsion ratio are higher for the first gear, it is the frequency at which the limiting value of unity is exceeded which fundamentally affects the rattle behaviour.

1.8- References

Azman, M., King, P.D. and Rahnejat, H., ''Combined bounce, pitch, and roll dynamics of vehicles negotiating single speed bump events'', *Proc. Instn. Mech. Engrs., Part K: J. Multi-body Dyn.*, *2007, **221(1)**, pp 33-40.*

Blundell, M.V., "The modelling and simulation of vehicle handling, Part 1: analysis methods", *Proc. Instn., Mech. Engrs., Part K: J. Multi-body Dyn., **213(2)**, 1999, pp. 103-118.*

Boysal, A. and Rahnejat, H., ''Torsional vibration analysis of a multi-body single cylinder internal combustion engine model'', *App. Math. Modelling*, *1997, **21**, pp. 481-493.*

Chandrasekhar, S., Newton's Principia, *Oxford University Press, Oxford, New York, 1995.*

Craig, R.R. Jr, Structural Dynamics: An Introduction to Computer Methods, *Soc. Exp. Mechs., Bethel, CT, USA, 1995.*

De la Cruz, M., Theodossiades, S., Rahnejat, H. and Kelly, P., "Impact dynamic behaviour of meshing loaded teeth in transmission drive rattle", *6th Euromech, Non-linear dynamics Conference, Saint Petersburg, Russia, 2008.*

De la Cruz, M., Theodossiades, S., Rahnejat, H. and Kelly, P.,"The effect of thermohydrodynamics on manual automotive transmissions gear rattle", *Proc. ASME, IDETC/CIE 2009, Pap. No. DETC2009-87226, San Diego, CA, USA, 2009a.*

De la Cruz, M., Theodossiades, S., Rahnejat, H. and Kelly, P., "Numerical and experimental analysis of manual automotive transmissions – gear rattle", *SAE Int., Pap.No. 2009-01-0328, 2009b.*

Gilmartin, G.M., "Constant velocity joints", *Engng., Feb. 1978, I-VIII.*

Gnanakumarr, G., Theodossiades, S., Rahnejat, H. and Menday, M., "Impact-induced vibration in vehicular driveline systems: theoretical and experimental investigations", *Proc. Instn. Mech. Engrs., Part K: J. Multi-body Dyn., 2005, **219**, pp. 1-12.*

Gohar, R., Elastohydrodynamics, *Imperial College Press, London, 2001.*

Rahnejat, H., “An introduction to multi-physics multi-scale approach”, in Rahnejat, H (Ed.), Tribology and dynamics of engine and power train, Woodhead Publishing, Cambridge, UK, 2010, ISBN: 978-1-84569-361-9

Gohar, R. and Rahnejat, H., Fundamentals of Tribology, *Imperial College Press, London, 2008.*

Greenwood, T.A. and Tripp, J.H., “The elastic contact of rough surfaces”, *Trans. ASME, J. Lubn. Tech., 1967, pp. 417.*

Grubin, A.N., “Contact stresses in toothed gears and worm gears”, *Book 30 CSRI for Tech. & Mech. Engng., Moscow, 1949, DSRI Trans., **37**.*

Hegazy, S., Rahnejat, H. and Hussain, K., "Multi-body dynamics in full-vehicle handling analysis under transient manoeuvre", *Vehicle System Dynamics*, *2000,**34**, pp 1-24.*

Houpert, L., “New results of traction force calculation in elastohydrodynamic contacts”, *Trans. ASME, J. Trib., **107**, 1985, pp. 241-248.*

Hunt, K.H., “Constant velocity shaft couplings: A general theory”, *Trans. ASME, J. Engng. Indust., 1973, pp. 455-464.*

Hussain, K., Rahnejat, H. and Hegazy, S., "Transient vehicle handling analysis with aerodynamic interactions", *Proc. Instn. Mech. Engrs., Part K: J. Multi-body Dyn.*, *2007, **221(1)**, pp. 21-32.*

Kushwaha, M., Gupta, S., Kelly, P. and Rahnejat, H., "Elasto-multi-body dynamics of a multi-cylinder internal combustion engine", *Proc. Instn. Mech. Engrs., Part K:Multi-body Dyn.*, *2002, **216**, pp 281-293.*

Nikravesh, P.E., “Newtonian-based methodologies in multi-body dynamics”, *Proc. Instn., Mech. Engrs., Part K: J. Multi-body Dyn., **222(4)**, 2008, pp. 277-288.*

Orlandea, N.V., “A study of the effect of lower index methods on ADAMS sparse tableau formulation for computational dynamics of multi-body mechanical systems”, *Proc. Instn., Mech. Engrs., Part K: J. Multi-body Dyn., **213(1)**, 1999, pp. 1-9.*

Orlandea, N.V., “From Newtonian dynamics to sparse tableaux formulation and multi-body dynamics”, *Proc. Instn., Mech. Engrs., Part K: J. Multi-body Dyn., **222(4)**, 2008, pp.301-314.*

Perera, M.S.M., Theodossiades, S. and Rahnejat, H., "A multi-physics multi-scale approach in engine design analysis", *Proc. Instn. Mech. Engrs., Part K: J. Multi-body Dyn., 2007, **221(3)**, pp. 335-348.*

Rahnejat, H., Multi-body Dynamics: Vehicles, Machines and Mechanisms, *Professional Engng. Publ. & SAE (Joint Publ.), Bury St Edmunds (UK) and Warrendale, Pa. (USA), 1998.*

Rahnejat, H., “An introduction to multi-physics multi-scale approach”, in Rahnejat, H (Ed.), Tribology and dynamics of engine and power train, Woodhead Publishing, Cambridge, UK, 2010, ISBN: 978-1-84569-361-9

Rahnejat, H., “Physics of causality and continuum: questioning Nature”, *Proc. Instn., Mech. Engrs., Part K: J. Multi-body Dyn., 2008, **222(4)**, pp. 255-264.*

Shabana, A.A., Dynamics of Multi-body Systems, *Cambridge University Press, 2005.*

Tangasawi, O.A.M., Theodossiades, S. and Rahnejat, H., "Gear teeth impacts in hydrodynamic conjunctions promoting idle gear rattle", *Journal of Sound and Vibration*, *2007, **303(3-5)**, pp 632-658.*